Supplemental Material - Salizzato et al.

Supplemental Figure Legends

Figure S1. Densitometric quantification of the immunostained protein bands shown in Fig. 1 and analysis of CK2 activity in WT and knockout C2C12 myoblasts. (*A*) Densitometric quantification of CK2α, CK2α' and CK2β protein amount in WT and knockout C2C12 myoblasts from immunostained bands obtained as in Fig. 1*A*, normalized to β-actin and relative to WT cells (n = 8 independent experiments; mean values ± SEM). *P < 0.05, ***P < 0.0001. (*B*) Phosphorylation extent of Akt1 Ser129 (p-Akt1 S129) quantified as the ratio of p-Akt1 Ser129/Akt1 immunostained bands obtained as in Fig. 1*A* and relative to WT cells (n = 8 independent experiments; mean values ± SEM). ***P < 0.0001. (*C*) CK2 kinase activity assayed *in vitro* towards the eIF2β(1-22) peptide-substrate in the cellular lysates of WT and knockout C2C12 myoblasts. Data are presented as percentage relative to WT myoblasts (n = 4 independent experiments; mean values ± SEM). **P <0.01, ***P < 0.0001. (*D*) Densitometric quantification of immunostained bands obtained as in Fig. 1*D*. Values are expressed relative to 2 d scrambled siRNA-treated (left panel) or 6 d scrambled siRNA- vehicle-treated (right panel) cells (n = 5 independent experiments at 2 d, n = 3 independent experiments at 6 d; mean values ± SEM). ***P < 0.0001. (*E*) Densitometric quantification of immunostained bands obtained as in Fig. 1*E*. Values are expressed relative to vehicle-treated cells (n = 4 independent experiments; mean values ± SEM). ***P < 0.0001.

Figure S2. Distribution of AchR clusters, quantification of the immunostained bands of Fig. 2*B* and *D*, comparison of CK2 tetramer amount in proliferating and differentiating WT cells and detection of CK2 kinase activity in WT and knockout C2C12 cells. (*A*) Representative confocal images of acetylcholine receptor (AchR) clustering in WT and knockout C2C12 myoblasts at 6 d of differentiation, stained with Alexa 555-conjugated Bungarotoxin (BTX) without (left images) or with (right images, Merge) light illumination to detect cell shape. (n = 3 independent experiments). Scale bar = 10 μm. (*B*) Densitometric quantification of the CK2α, CK2α', CK2β and MyoD protein amount in differentiating WT and knockout cells from immunostained bands obtained as in Fig. 2*B* and *D* at the indicated time points, normalized to β-actin and relative to WT proliferating (0 d) cells (n = 5 independent experiments; mean values ± SEM). (*C*) Representative immunoblotting of CK2α, CK2α' or CK2β immunoprecipitates from proliferating (0 d) or differentiated (6 d) WT C2C12 cells (n = 4). (*D*) Phosphorylation of Akt1 Ser129 (p-Akt1 S129) quantified as the ratio of p-Akt1 Ser129/Akt1 immunostained bands obtained as in Fig. 2*D* (n = 5 independent experiments; mean values ± SEM). (*E*) CK2 kinase activity assayed *in vitro* using the eIF2β(1-22) peptide-substrate in

the cellular lysates of differentiating WT and knockout C2C12 cells. Data are percentage relative to WT proliferating (0 d) myoblasts (n = 4 independent experiments; mean values ± SEM). (*B, D, E*) Statistical significance for knockout cells *versus* WT cells was calculated at each time point by two-way ANOVA, followed by Bonferroni's multiple comparison test $^{\#}P < 0.05$, $^{\#\#}P < 0.01$, $^{\#\#\#}P < 0.001$. Two-tailed Student's t-test was used to assess the statistical significance of differentiating *versus* proliferating cells (0 d). $^{**}P < 0.01$, $^{***}P < 0.0001$.

Figure S3. Analysis of cell migration, cytoskeletal remodeling and fusogenic protein translocation in WT and CK2α'$^{-/-}$ C2C12 cells. (*A*) Representative images of cell migration assessed by wound healing assay in proliferating WT or CK2α'$^{-/-}$ C2C12 cells at 0, 14 and 18 h (n = 3). (*B*) Cell migration was quantified in images obtained as in *A* by measuring the scratch-area covered by cells at the indicated time point and expressed as the percentage of the scratch-area at 0 h. (*C*) Representative confocal images of proliferating WT or CK2α'$^{-/-}$ C2C12 cells stained with phalloidin (red) or α-tubulin antibody (green) (n = 4 independent experiments). (*D*) Densitometric quantification of caveolin-3 and myomixer protein amount in the plasma membrane fraction (PM) of differentiating WT or CK2α'$^{-/-}$ cells. Values, acquired from the immunostained bands obtained as in Fig. 2*I*, were normalized to the plasma membrane Ca^{2+} ATPase (PMCA) bands and relative to WT cells. (n = 4 independent experiments; mean values ± SEM). $^{***}P < 0.0001$.

Figure S4. Dose- and time-dependent inhibition of C2C12 myoblast differentiation, muscle-specific protein expression and fusogenic protein translocation by CX-5011. (*A-D*) WT C2C12 cells, differentiated for 6 d in the presence of vehicle or the indicated concentrations of CX-5011, were lysed and lysate proteins were analyzed. (*A*) Immunoblotting analysis with the indicated antibodies. β-actin was used as loading control. (n = 3 independent experiments). (*B*) CK2 kinase activity assayed *in vitro* using the eIF2β(1-22) peptide-substrate. Data are expressed as percentage relative to vehicle-treated cells (n = 3 independent experiments; mean values ± SEM). $^{***}P < 0.0001$. (*C*) Cell viability measured by MTT assay of C2C12 cells at 6 d of differentiation. Data are expressed as percentage relative to vehicle-treated cells (n = 3 independent experiments; mean values ± SEM). (*D*) Cellular morphology assessed by bright field microscopy (n = 3 independent experiments). (*E*) Densitometric quantification of CK2α, CK2α' and CK2β protein amount from immunostained bands obtained as in Fig. 3*A* and normalized to β-actin (n = 5 independent experiments; mean values ± SEM). $^{*}P < 0.05$, $^{***}P < 0.0001$ *versus* vehicle-treated cells at 2 h. (*F*) Phosphorylation of Akt1 Ser129 (p-Akt1 S129) quantified as the ratio of p-Akt1 Ser129/Akt1 immunostained bands obtained as in Fig. 3*A* (n = 5 independent experiments; mean values ± SEM). $^{**}P < 0.01$, $^{***}P < 0.001$ *versus*

vehicle-treated cells at 2 h. (*G*) CK2 kinase activity of cellular lysates from vehicle- or CX-5011-treated differentiating C2C12 myoblasts, assayed *in vitro* using the eIF2β(1-22) peptide-substrate. Data are percentage of vehicle-treated cells at 2 h (n = 3 independent experiments; mean values ± SEM). ***P < 0.0001. (*H*) Densitometric quantification of muscle differentiation marker protein amount from immunostained bands obtained as in Fig. 3*C*, normalized to β-actin and expressed relative to vehicle-treated cells at 3 d (n = 5 independent experiments; mean values ± SEM). *P < 0.05, **P < 0.01, ***P < 0.0001 for CX-5011- *versus* vehicle-treated cells at each time point. (*I*) Densitometric quantification of MyoD and myogenin protein amount from immunostained bands obtained as in Fig. 3*C*, normalized to β-actin and expressed relative to vehicle-treated C2C12 cells at 2 h (n = 5 independent experiments; mean values ± SEM). (*J*) Densitometric quantification of caveolin-3 and myomixer protein amount in the plasma membrane fraction (PM) of differentiating WT cells treated with vehicle or 2 μM CX-5011 at 4 d. Values, acquired from the immunostained bands obtained as in Fig. 3*J*, were normalized to the plasma membrane Ca^{2+} ATPase (PMCA) bands and relative to vehicle-treated cells. (n = 4 independent experiments; mean values ± SEM). ***P < 0.0001. (*K*) Cellular morphology assessed by bright field microscopy of differentiating C2C12 cells in the presence of vehicle or 2 μM CX-5011 for the indicated time windows and analyzed at 6 d. In the case of CX-5011-treatment for the first day (0-1 d), the medium was replaced after 1 d with the conditioned medium of vehicle-treated C2C12 cells at 1 d of differentiation.

Figure S5. Inhibition of CK2 activity impairs CK2α'$^{-/-}$ C2C12 cell differentiation. CK2α'$^{-/-}$ C2C12 cells were differentiated in the presence of vehicle or 2 μM CX-5011 and analyzed at 6 d of differentiation. (*A*) Cellular morphology assessed by bright field microscopy (n = 3 independent experiments). Scale bar, 200 μm. (*B*) Immunoblotting analysis of cellular lysates with the indicated antibodies. β-actin was used as loading control (n = 3 independent experiments). (*C*) Densitometric quantification of the immunostained bands obtained as in *B*, normalized to β-actin and expressed relative to vehicle-treated cells (n = 3 independent experiments; mean values ± SEM). ***P < 0.0001.

Figure S6. Inhibition of CK2 activity impairs the expression of myogenic markers and myoblast fusion in regenerating mouse muscle and developing zebrafish embryo. Overexpression of CK2α' stimulates C2C12 cell fusion. (*A*) Densitometric quantification of the immunostained bands obtained as in Fig. 5*B*, normalized to β-actin and expressed relative to vehicle-treated muscles (n = 7 mice; mean values ± SEM). ***P < 0.0001. (*B*) Representative bright field images of hematoxylin and eosin staining of transversal cryosections from regenerating mouse tibialis anterior (TA) muscles

treated with vehicle or CX-5011 at the indicated time points after cardiotoxin injury. Scale bar, 50 μm. (*C*) Representative images of TA muscle sections immunostained with anti-Pax7 or anti-MyoD (red) and anti-laminin (green) antibodies at 4 d of regeneration. Hoechst (blue) stains nuclei (n = 4 mice). Scale bar, 10 μm. (*D*) Densitometric quantification of the immunostained bands obtained as in Fig. 5*J*, normalized to β-actin and expressed relative to empty vector-transfected muscles (n = 3 mice; mean values ± SEM). ***P < 0.0001. (*E*) Immunofluorescence of C2C12 cells co-transfected with pEGFP-N1 + pcDNA3.1 (empty) or pEGFP-N1 + pRcCMV2-CK2α'-HA (CK2α') plasmids and stained with anti-troponin T antibody (green) at 2 d of differentiation. Transfected cells are identified by GFP fluorescence pseudo-colored in red. Hoechst (blue) stains nuclei (n = 3). Scale bar, 10 μm. (*F*) Quantification of mononucleated GFP- and troponin T-double positive cell number from images obtained as in *E*, expressed as percentage over the total GFP- and troponin T-double positive cells (n = 3; mean values ± SEM). ***P < 0.0001. (*G*) Fusion index, defined as the percentage of nuclei present in transfected GFP- and troponin T-double positive myotubes over the total number of nuclei of transfected cells in images as in *E*, where cells containing at least 3 nuclei are considered myotubes (n = 3; mean values ± SEM). ***P < 0.0001. (*H*) Representative confocal images showing the lateral view (anterior to the left) of 48 hpf zebrafish tail somites, immunostained for fast fiber-type-specific myosin (F310 antibody, green) and counterstained with Hoechst (blue) to detect nuclei. Scale bar, 10 μm. (*I*) Fiber myonuclei content in 48 hpf zebrafish embryo tail somites measured in images obtained as in *H*. Data are presented as percentage of fibers with the indicated number of nuclei over the total number of fibers considered (n = 354 fibers from vehicle-treated and n = 314 fibers from CX-5011-treated embryos, mean values ± SEM). ***P < 0.0001 *versus* fibers from vehicle-treated embryos. (*J*) Representative confocal images showing the lateral view (anterior to the left) of 96 hpf zebrafish tail somites, immunostained for fast fiber-type-specific myosin (F310 antibody, green) and counterstained with Hoechst (blue) to detect nuclei. Scale bar, 10 μm. (*K*) Fiber myonuclei content in 96 hpf zebrafish embryo tail somites measured in images obtained as in *J*. Data are presented as percentage of fibers with the indicated number of nuclei over the total number of fibers considered (n = 329 fibers from vehicle-treated and n = 370 fibers from CX-5011-treated embryos, mean values ± SEM). ***P < 0.0001 *versus* fibers from vehicle-treated embryos.

Supplemental Figures

Fig. S1

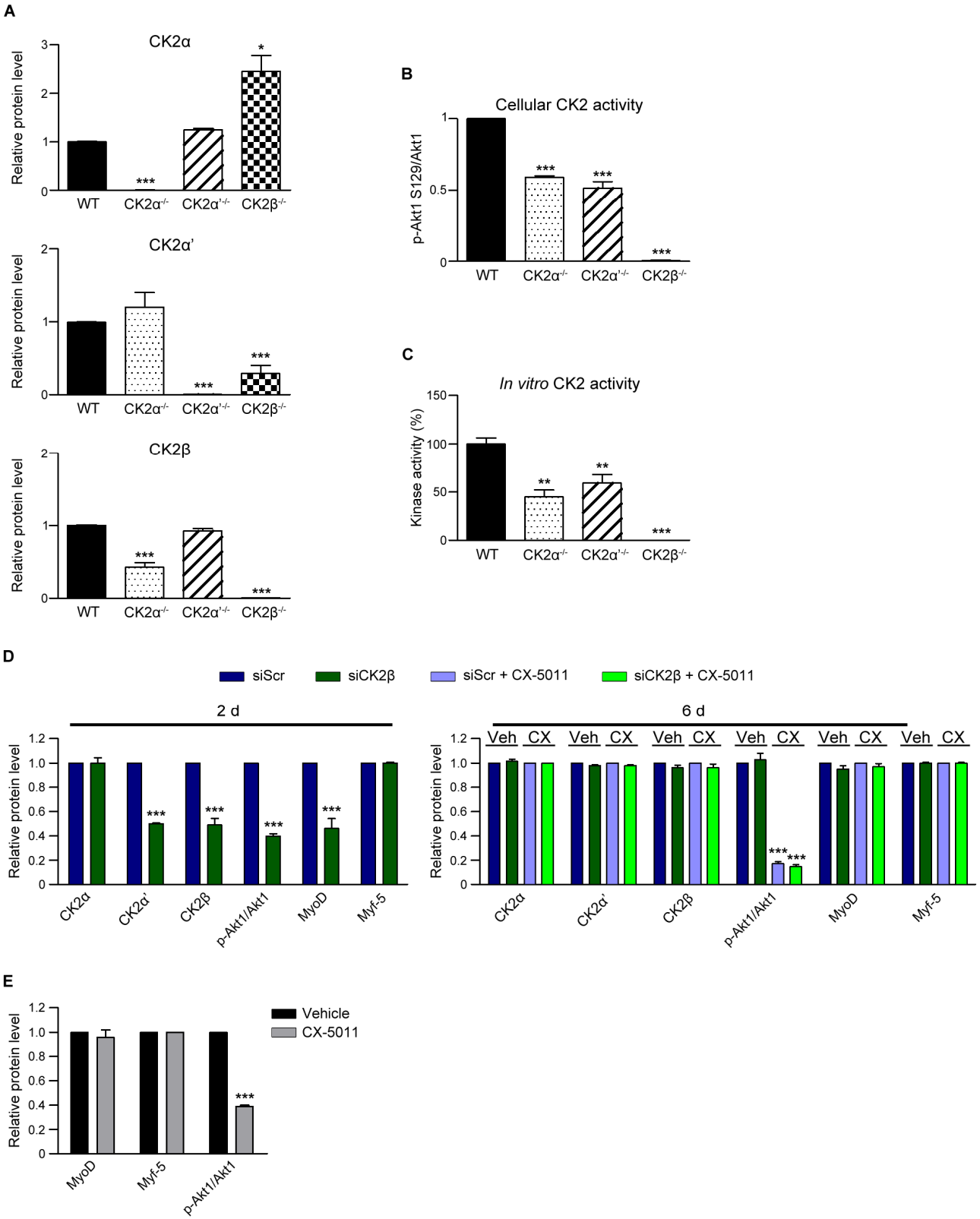

Fig. S2

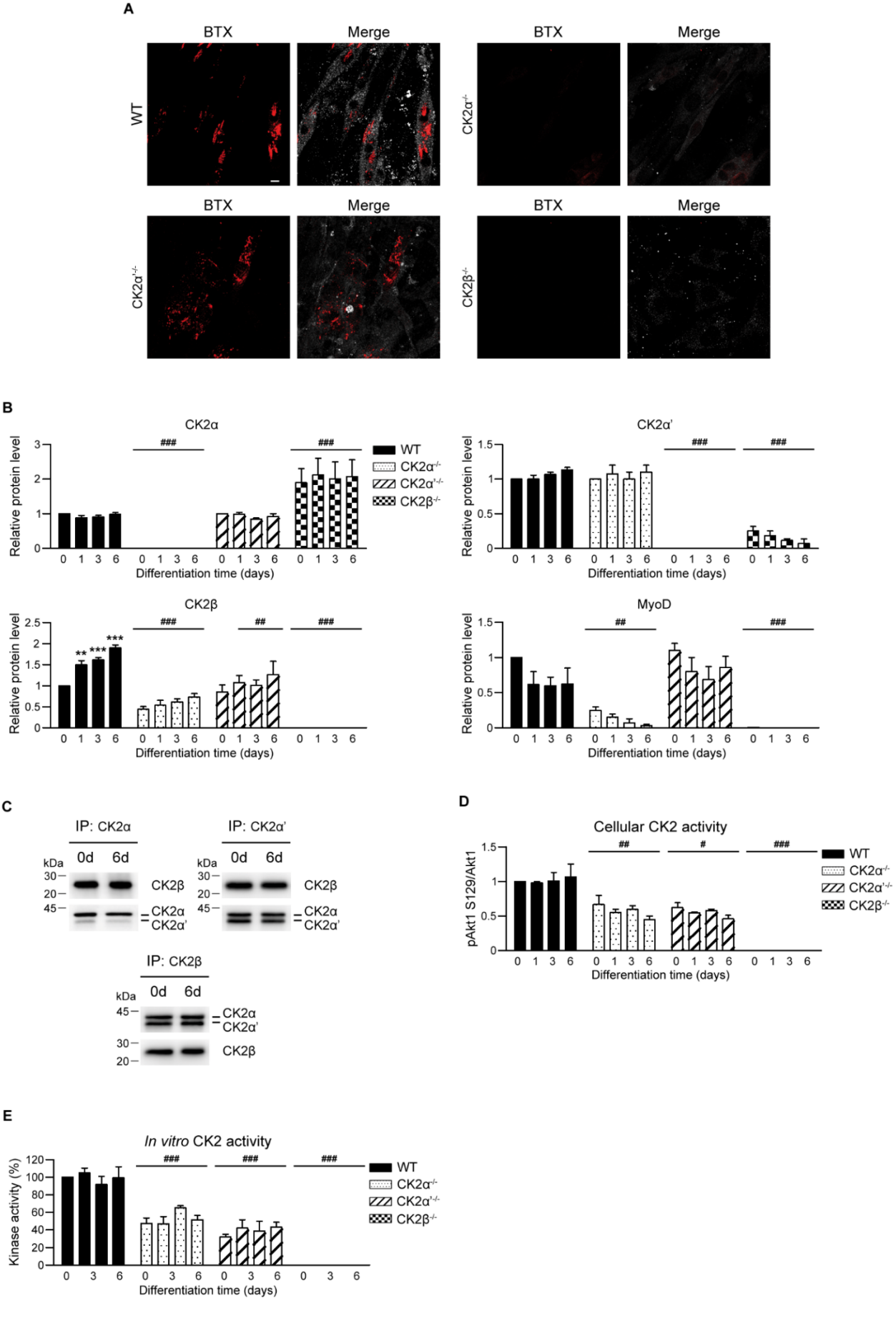
A
BTX
Merge
WT
CK2α-/-
CK2α'-/-
CK2β-/-
B
CK2α
CK2α'
CK2β
MyoD
Relative protein level
Differentiation time (days)
WT
CK2α-/-
CK2α'-/-
CK2β-/-
C
IP: CK2α
IP: CK2α'
IP: CK2β
kDa
0d
6d
CK2β
CK2α
CK2α'
D
Cellular CK2 activity
pAkt1 S129/Akt1
E
In vitro CK2 activity
Kinase activity (%)

Fig. S3

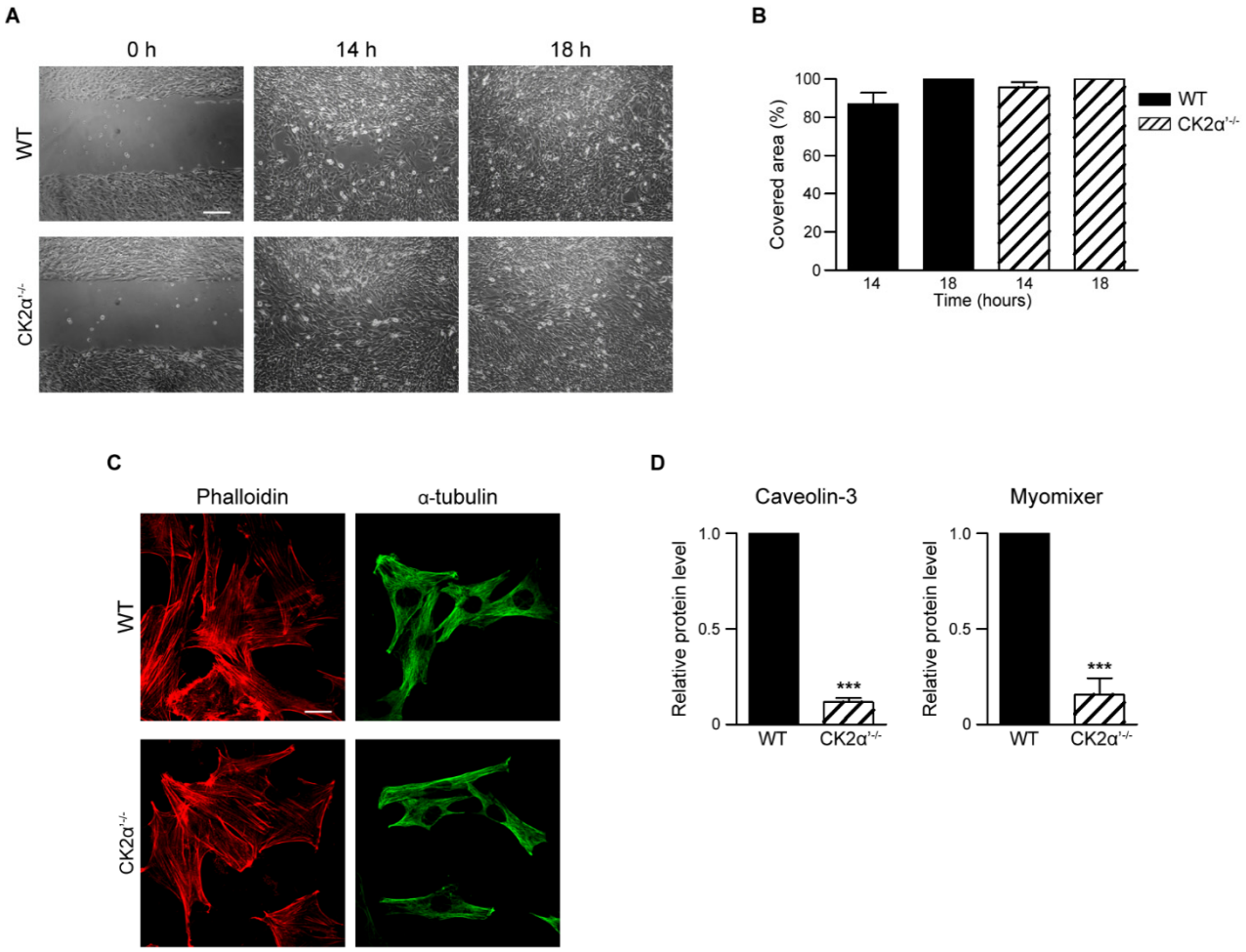
A
0 h
14 h
18 h
WT
CK2α-/-
B
Covered area (%)
100
80
60
40
20
0
14
18
14
18
Time (hours)
WT
CK2α-/-
C
Phalloidin
α-tubulin
WT
CK2α-/-
D
Caveolin-3
Myomixer
Relative protein level
1.0
0.5
0
***
WT
CK2α-/-

Fig. S4

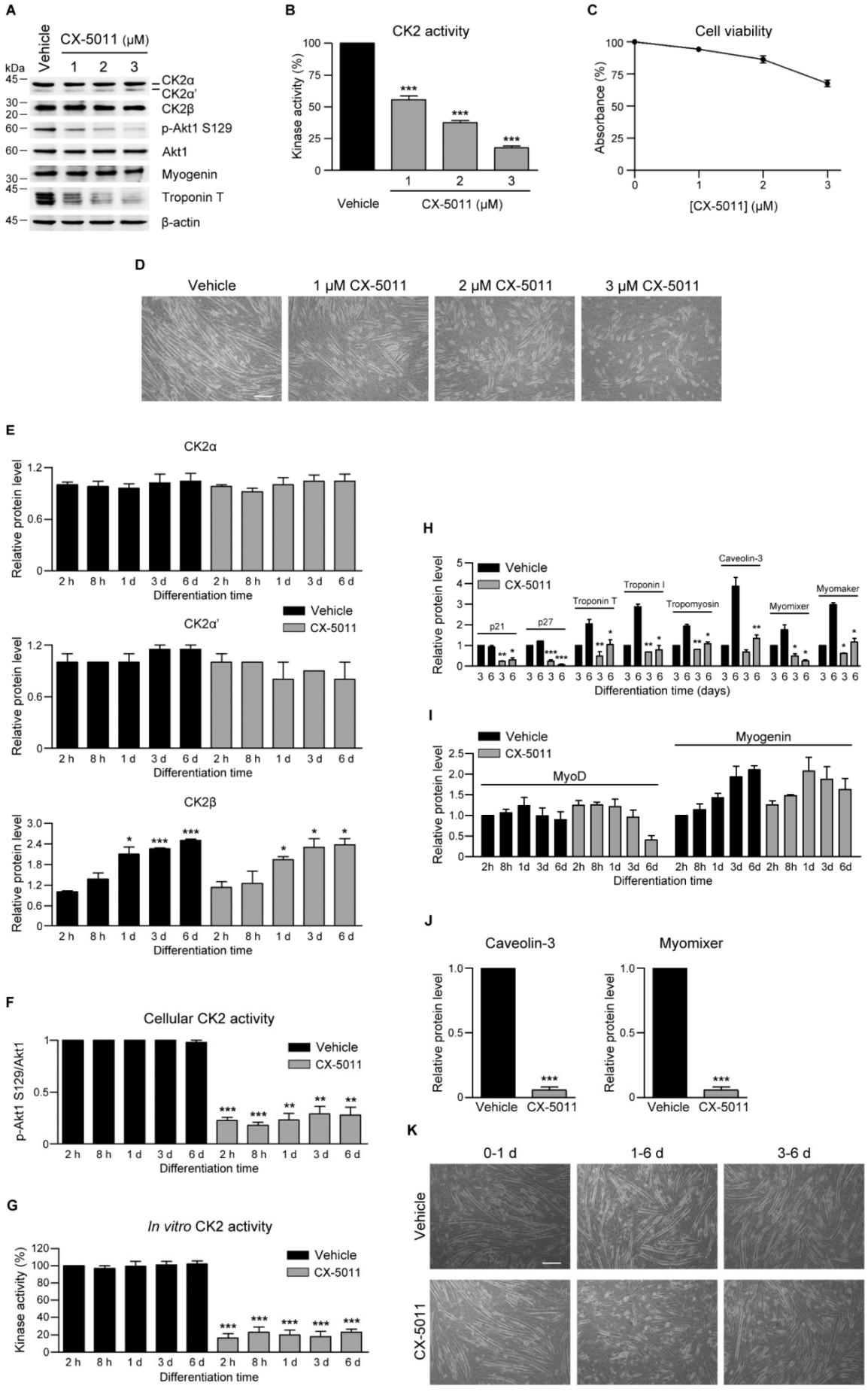
A
Vehicle
CX-5011 (μM)
1
2
3
kDa
45
CK2α
CK2α'
30
20
CK2β
60
p-Akt1 S129
60
Akt1
30
Myogenin
45
Troponin T
45
β-actin
B
CK2 activity
Kinase activity (%)
100
75
50
25
0
***
***
***
1
2
3
Vehicle
CX-5011 (μM)
C
Cell viability
Absorbance (%)
100
75
50
25
0
0
1
2
3
[CX-5011] (μM)
D
Vehicle
1 μM CX-5011
2 μM CX-5011
3 μM CX-5011
E
CK2α
Relative protein level
1.2
0.6
0
2 h
8 h
1 d
3 d
6 d
Differentiation time
Vehicle
CX-5011
CK2α'
CK2β
F
Cellular CK2 activity
p-Akt1 S129/Akt1
Differentiation time
G
In vitro CK2 activity
Kinase activity (%)
120
100
80
60
40
20
0
H
Relative protein level
p21
p27
Troponin T
Troponin I
Tropomyosin
Caveolin-3
Myomixer
Myomaker
3 6 3 6
Differentiation time (days)
I
MyoD
Myogenin
2h 8h 1d 3d 6d 2h 8h 1d 3d 6d
Differentiation time
J
Caveolin-3
Myomixer
Relative protein level
1.0
0.5
0
***
Vehicle
CX-5011
K
0-1 d
1-6 d
3-6 d
Vehicle
CX-5011

Fig. S5

A

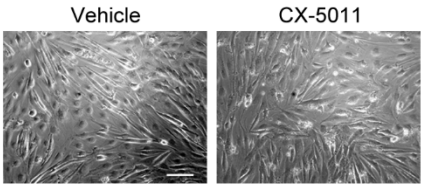
Vehicle
CX-5011

B

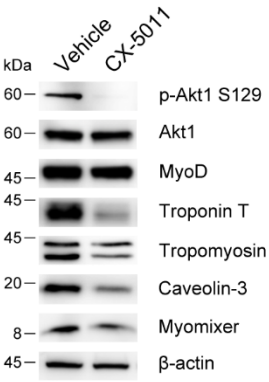
kDa
Vehicle
CX-5011
60
p-Akt1 S129
60
Akt1
45
MyoD
45
Troponin T
45
Tropomyosin
20
Caveolin-3
8
Myomixer
45
β-actin

C

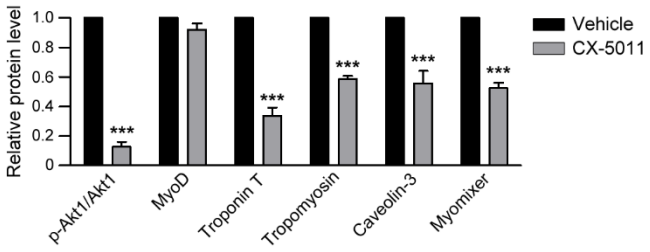
Relative protein level
1.0
0.8
0.6
0.4
0.2
0
***
p-Akt1/Akt1
MyoD
Troponin T
Tropomyosin
Caveolin-3
Myomixer
Vehicle
CX-5011

Fig.S6

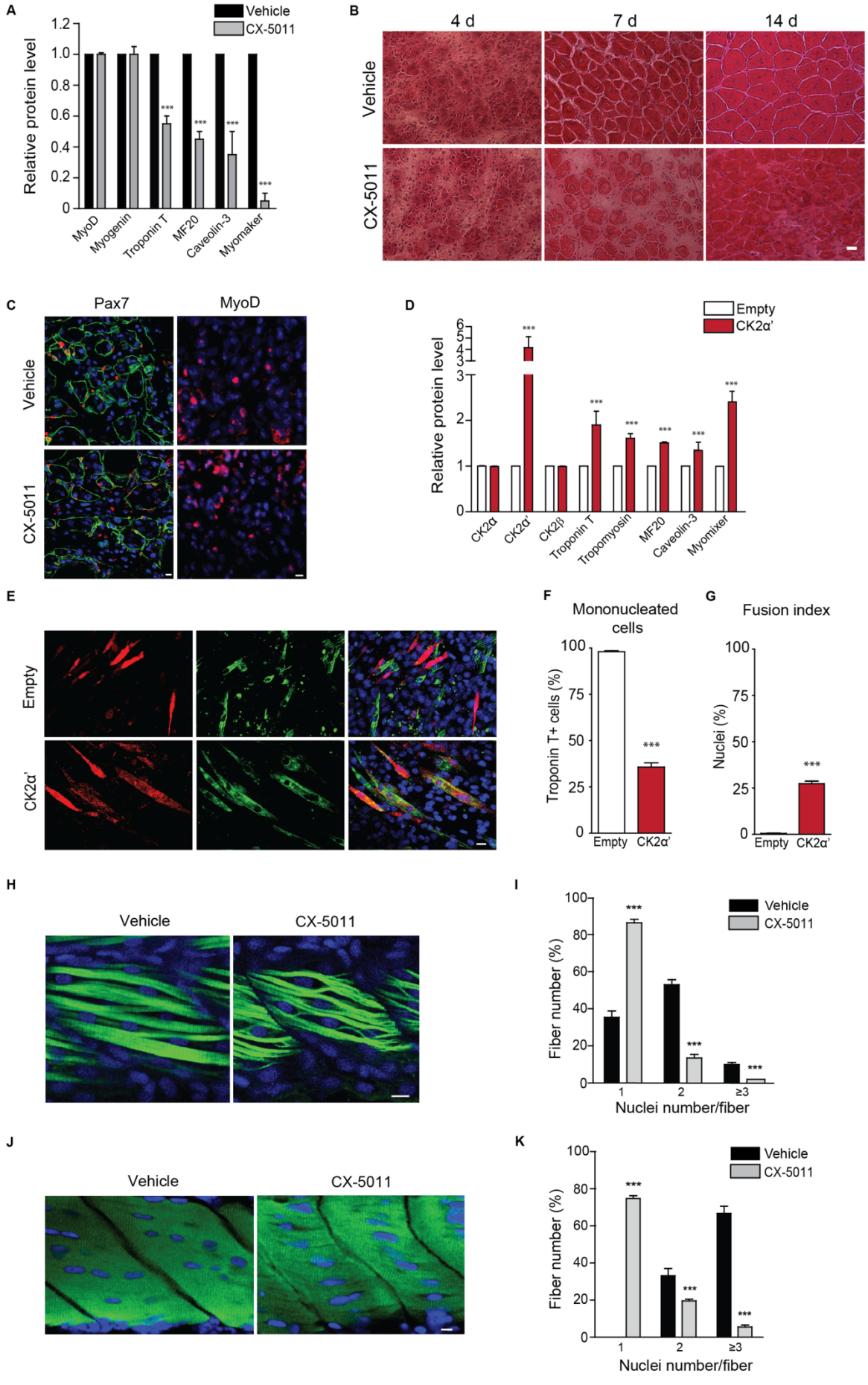
A
Vehicle
CX-5011
Relative protein level
MyoD
Myogenin
Troponin T
MF20
Caveolin-3
Myomaker
B
4 d
7 d
14 d
Vehicle
CX-5011
C
Pax7
MyoD
Vehicle
CX-5011
D
Empty
CK2α'
Relative protein level
CK2α
CK2α'
CK2β
Troponin T
Tropomyosin
MF20
Caveolin-3
Myomixer
E
Empty
CK2α'
F
Mononucleated cells
Troponin T+ cells (%)
Empty
CK2α'
G
Fusion index
Nuclei (%)
Empty
CK2α'
H
Vehicle
CX-5011
I
Vehicle
CX-5011
Fiber number (%)
Nuclei number/fiber
J
Vehicle
CX-5011
K
Vehicle
CX-5011
Fiber number (%)
Nuclei number/fiber